Electrical properties of the titanium acceptor in silicon carbide

Thomas Dalibor and Gerhard Pensl
Institute of Applied Physics, University of Erlangen-Nürnberg, Staudtstraße 7, D-91058 Erlangen, Germany

Nils Nordell and Adolf Schöner
Industrial Microelectronics Center, P.O. Box 1084, S-16421 Kista/Stockholm, Sweden

(Received 14 August 1996; revised manuscript received 15 January 1997)

The transition-metal titanium (Ti) as an extrinsic impurity in the wide-band-gap semiconductor silicon carbide (SiC) is studied, applying deep-level transient spectroscopy on Ti^+-implanted $4H$ and $6H$ SiC epitaxial layers. Two Ti centers with energy positions $E_C-(117\pm8)$ meV and $E_C-(160\pm10)$ meV, respectively, are observed in the $4H$ polytype. These levels are assigned to the ionized Ti acceptor $Ti^{3+}(3d^1)$ residing at hexagonal and cubic Si lattice sites. For the $6H$ SiC polytype, the Ti acceptor levels are assumed to be resonant in the conduction band. [S0163-1829(97)06320-0]

I. INTRODUCTION

The wide-band-gap semiconductor silicon carbide (SiC) is considered to replace silicon (Si) in the field of high-temperature, high-frequency, and high-power devices. With respect to these applications, the use of Si is limited due to its physical properties, which are summarized in ''figures of merit'' (see, e.g., Refs. 1–4). One of the most striking features of SiC is the existence of many stable modifications, so-called polytypes, differing only in the stacking sequence of periodic Si-C double layers along the c axis. The various polytypes have different indirect band-gap energies ranging from 2.3 eV for $3C$ to 3.35 eV for $2H$ SiC at room temperature. The most relevant polytypes with respect to device applications are $4H$ and $6H$ SiC with band-gap energies at room temperature of 3.28 and 3.08 eV, respectively. Depending on the particular polytype, several inequivalent lattice sites can be distinguished, e.g., one cubic (k) and one hexagonal (h) in $4H$ and two cubic (k_1,k_2) and one hexagonal (h) in $6H$ SiC.

Epitaxial layers, which are grown by the chemical vapor deposition (CVD) technique,[5,6] are used for the fabrication of electronic devices. The graphite parts employed in such growth facilities contain a considerable amount of transition-metal impurities, e.g., titanium (Ti), which may lead to a degradation of electronic devices.

Ti is incorporated into the SiC lattice either substitutionally as an isolated atom, or it tends to form TiN pairs;[7,8] although there were copious amounts of nitrogen in our SiC samples, TiN pairs, which have a ground level of about 600 meV below the conduction-band edge in $6H$ SiC,[8] were not observed in the studies of this paper. Optically detected magnetic resonance (ODMR) investigations established that Ti substitutes for Si at the differing inequivalent lattice sites, and forms an isoelectronic center $[Ti^{4+}(3d^0)]$.[9] Patrick and Choyke (see Ref. 10 and references therein) performed detailed low-temperature photoluminescence investigations on isoelectronic Ti centers in different SiC polytypes ($4H$, $6H$, $8H$, $15R$, $21R$, $33R$, and $3C$). The authors proposed that the observed photoluminescence (PL) is caused by the radiative recombination of an exciton bound to the Ti center.

The isoelectronic Ti center is found to act as an acceptor with a stable ionized state according to $Ti^{3+}(3d^1)/Ti^{4+}(3d^0)\equiv A^-/A^0$. The excited state A^- provides a spin which is equal to $\frac{1}{2}$; this state could be detected in n-type $4H$ SiC with the electron-spin-resonance (ESR) technique; however, it was not detectable in n-type $6H$ SiC.[8] Although nothing was known about the energy position of the A^- center, it was speculated that the A^- state lies resonant in the conduction band of the $6H$ polytype.[8]

It is, therefore, the aim of this paper to determine experimentally the ground-state levels of the ionized Ti acceptor. For that reason, n-type $4H$ and $6H$ SiC CVD-grown epitaxial layers were implanted with Ti and analyzed by deep-level transient spectroscopy (DLTS). For comparison, an implantation with a corresponding vanadium (V) profile was carried out to distinguish between implantation-induced and Ti-related defect centers, because Ti and V are of similar masses and, therefore, should yield a comparable damage profile. Two Ti-related centers are observed in the DLTS spectra of n-type $4H$ SiC samples; they are attributed to ionized Ti acceptors residing at hexagonal and cubic Si lattice sites in agreement with ESR (Ref. 8) and ODMR (Ref. 9) results given in the literature. We could not detect any corresponding ground levels in the $6H$ polytype. Based on our DLTS studies and on published ESR (Ref. 8) and PL (Ref. 10) data, the appearance of ground levels of the ionized Ti acceptor in the band gap of different SiC polytypes and the binding energy of an exciton bound to the Ti acceptor are discussed.

II. EXPERIMENT

The $4H$ and $6H$ SiC epilayers used for these investigations were simultaneously grown by CVD in a silane (SiH_4)–propane (C_3H_8)–hydrogen (H_2) system on n-type $4H$ and $6H$ SiC {0001} substrates, respectively.[5] The growth temperature was 1620 °C, and the C/Si ratio in the source gas flow was equal to 1.5. For capacitance-voltage (C-V)and DLTS measurements, we prepared nickel (Ni)

TABLE I. Implantation parameters used for the two sets of Ti^+ implantation and the one set of V^+ implantation. E is equal to acceleration and Φ is equal to fluence.

	Ti^+ implantation No. 1	Ti^+ implantation No. 2	V^+ implantation
1	$E=1.9$ MeV $\Phi=1.4\times10^{11}$ cm^{-2}	$E=1.9$ MeV $\Phi=6.8\times10^{11}$ cm^{-2}	$E=1.9$ MeV $\Phi=1.4\times10^{11}$ cm^{-2}
2	$E=1.3$ MeV $\Phi=1.0\times10^{11}$ cm^{-2}	$E=1.3$ MeV $\Phi=5.2\times10^{11}$ cm^{-2}	$E=1.3$ MeV $\Phi=1.0\times10^{11}$ cm^{-2}
3	$E=800$ keV $\Phi=8.8\times10^{10}$ cm^{-2}	$E=800$ keV $\Phi=4.4\times10^{11}$ cm^{-2}	$E=800$ keV $\Phi=8.8\times10^{10}$ cm^{-2}
4	$E=450$ keV $\Phi=6.8\times10^{10}$ cm^{-2}	$E=450$ keV $\Phi=3.4\times10^{11}$ cm^{-2}	$E=450$ keV $\Phi=6.8\times10^{10}$ cm^{-2}
$\Phi_{integral}$	4×10^{11} cm^{-2}	2×10^{12} cm^{-2}	4×10^{11} cm^{-2}
Mean concentration of implanted ion species	4×10^{15} cm^{-3}	2×10^{16} cm^{-3}	4×10^{15} cm^{-3}

Schottky contacts with a diameter of 0.7 mm on top of the epilayers using an electron-beam evaporation system. Large-area Ohmic contacts were fabricated on the backside of the substrates by evaporating Ni. C-V measurements revealed a net donor concentration N_D-N_A of the as-grown epilayers of about $(1-3)\times10^{16}$ cm^{-3}. Selected 4H and 6H SiC epilayers were implanted with Ti. In order to achieve a rectangular profile to a depth of 1.2 μm, we conducted a fourfold implantation with an integral fluence of 4×10^{11} cm^{-2} (implantation No. 1) and 2×10^{12} cm^{-2}(implantation No. 2), respectively (for parameters of the individual Ti^+ implantations, see Table I). An identical V profile with an integral fluence of 4×10^{11} cm^{-2}was implanted for comparison (see Table I). Subsequent to the implantation the epilayers were annealed at 1700 °C for 30 min to reduce the implantation damage and to electrically activate the implanted ion species. The anneals were performed in a furnace with a closed SiC crucible under argon atmosphere to avoid thermal decomposition of the sample surfaces. A fast computer-controlled DLTS system[11] was used to carry out DLTS measurements in a temperature range from 30 to 300 K with a reverse bias of -4 V, a filling pulse bias of -0.5 V, and a filling pulse width of 20 ms.

III. EXPERIMENTAL RESULTS AND DISCUSSION

Figure 1 depicts normalized DLTS spectra $[C(t_2)-C(t_1)]/(x_r-x_p)$ (x_r is the space-charge width at reverse bias V_r, $x_p$is the space-charge width at filling pulse bias V_p, and the time window $t_1=1$ ms/$t_2=2$ ms) taken on the as-grown, the Ti^+-implanted (implantation No. 1), and the V^+-implanted 4H SiC epilayers. Seven pronounced peaks can be observed in the DLTS spectrum of the Ti^+-implanted sample (solid curve) within a temperature range from 30 to 240 K. The four peaks termed ID_1 to ID_4 appear in the DLTS spectrum of the Ti^+ as well as of the V^+-implanted samples; they can consequently not be related to Ti. These peaks are assigned to implantation-induced intrinsic defect centers. The ground level of the vanadium acceptor appears at $T\approx520$ K (at $T\approx400$ K in 6H SiC) with an ionization energy which agrees well with resistivity and DLTS measurements reported in Ref. 12; this higher-temperature part of the DLTS spectrum, however, is cut off in Fig. 1, because the emphasis of this paper is focused on Ti levels which appear in the depicted temperature range. The peak labeled N(k) in Fig. 1 is due to the nitrogen (N) donor residing at cubic carbon lattice sites. This assignment is based on the temperature position of the peak maximum at $T\approx50$ K (see Ref. 13). At this temperature, N donors N(h) residing at hexagonal carbon lattice sites serve as a source for the free electrons in the conduction band, which are required to be able to conduct DLTS measurements. N(h)donors are present at identical concentration as N(k) donors [N(N(h)]=N(N(k))] in the 4H polytype and have a smaller ionization energy than N(k) donors (for ionization energies of N donors, see Ref. 14).

This conclusion is supported by C-V measurements conducted on the same samples. Curves 1–3 in Fig. 2 are taken on as-grown, Ti^+-implanted, and V^+-implanted samples.

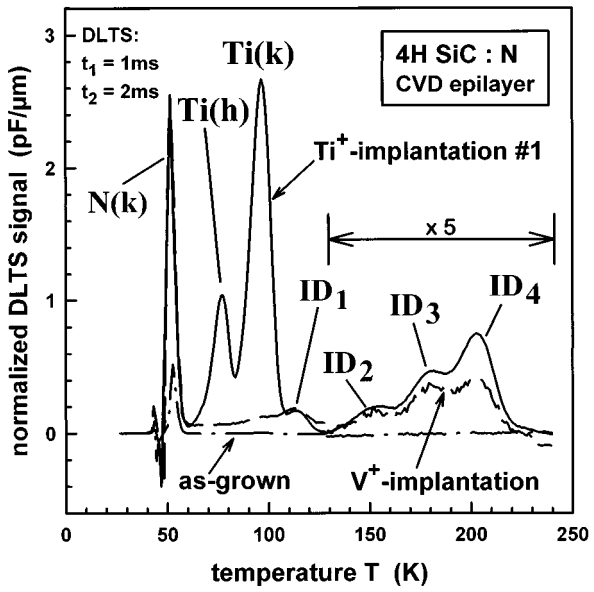

FIG. 1. Normalized DLTS spectrum (time window $t_1=1$ ms/$t_2=2$ ms) of an as-grown (dot-dashed curve), of a Ti^+-implanted (implantation No. 1, solid curve) and of a V^+-implanted (dashed curve) 4H SiC epilayer. The implanted epilayers were annealed at 1700 °C for 30 min. The normalized DLTS spectra are magnified by a factor of 5 in the temperature range from 130 to 240 K.

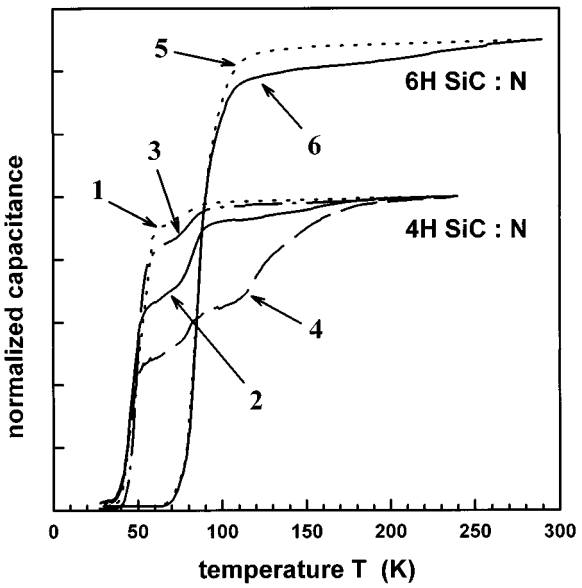

FIG. 2. Normalized capacitance over temperature as obtained from C-V measurements (frequency 1 MHz). The C-T curves are taken (1) on an as-grown 4H SiC sample (dotted curve), (2) on a 4H SiC sample subsequent to the Ti^+ implantation No. 1 (solid curve), (3) on a 4H SiC sample subsequent to the V^+ implantation (dot-dashed curve), (4) on a 4H SiC sample subsequent to the Ti^+ implantation No. 2 (dashed curve), (5) on an as-grown 6H SiC sample (dotted curve), and (6) on a 6H SiC sample subsequent to the Ti^+ implantation No. 1 (solid curve). All the implanted SiC samples were, in addition, exposed to an anneal at 1700 °C for 30 min.

All three C-T curves show a freeze-out of free electrons in the conduction band at a few degrees below 50 K. Therefore, N(k) donors are observable in the DLTS spectra; however, the low-temperature edge of the corresponding peak is affected by the steep freeze-out. Consequently, an Arrhenius analysis of this center can no longer be conducted.

The two peaks at $T \approx 75$ K [Ti(h)] and $T \approx 95$ K [Ti(k)] in Fig. 1 could only be observed in Ti^+-implanted 4H SiC epilayers; they are assumed to be due to Ti atoms residing at hexagonal and cubic Si lattice sites, respectively.[9] We would like to point out that these two peaks are also detectable in the as-grown epilayer, though at a small concentration of about 1×10^{13} cm^{-3}, which is no longer observable using the scale of Fig. 1. The ionization energies $\Delta E(i)$, capture cross sections $\sigma(i)$ of electrons and concentrations N(i) of centers Ti(h), Ti(k), and ID_1–ID_4 obtained from an Arrhenius plot evaluation, are listed in Table II. Because of the fact that the temperature dependence of the capture cross section of electrons is unknown, we used the following two cases for the Arrhenius analysis: $\sigma \sim T^0$ (multiphonon capture) and $\sigma \sim T^{-2}$ (cascade capture). For the Ti-related peaks Ti(h) and Ti(k), we determined averaged ionization energies (for values assuming $\sigma \sim T^0$ and $\sigma \sim T^{-2}$; see Table II) of $\Delta E[\mathrm{Ti}(h)] = (117 \pm 8)$ meV and $\Delta E[\mathrm{Ti}(k)] = (160 \pm 10)$ meV, respectively. Assuming identical occupation probabilities for hexagonal (h) and cubic (k) lattice sites in the 4H SiC polytype, we would expect identical concentrations of Ti(h) and Ti(k) centers. As can be seen in the last column of Table II, the concentration of Ti(h) centers evaluated from DLTS data (for the calculation of the concentration, see, e.g., Refs. 15 and 16) is reduced by approximately a factor of 2. This reduction is caused by a partial freeze-out of free electrons in the conduction band which means by trapping free electrons in energetically deeper impurities (Ti acceptor levels) and lowering the effective doping level, as can be observed in the C-T curves of Fig. 2. The determination of the concentration of Ti(k) centers, however, is not affected by the charge-carrier freeze-out.

In order to check whether the measured concentration of Ti centers [Ti(h), Ti(k)] correlates with the concentration of the implanted rectangular Ti profile, we conducted a second implantation (Ti^+ implantation No. 2) with a fluence five times higher. At first sight, the measured concentrations of Ti centers [Ti(h), Ti(k)] do not meet the expectations, because the peak heights of Ti(h) and Ti(k) in the corresponding DLTS spectra in Fig. 3 are by factors of 1.5 and 2.4, smaller and higher, respectively, than in samples exposed to Ti^+ implantation No. 1. Also, peak N(k) is reduced in its height. In the case of Ti^+ implantation No. 2 the freeze-out of free electrons is much stronger, and occurs between 70 and 140 K, as can be seen from the dashed curve 4 in Fig. 2. A corresponding freeze-out behavior is not observed in as-grown (dotted curve 1) or V^+-implanted (dot-dashed curve 3) samples. The freeze-out in the temperature range from 50 to 140 K is obviously enhanced by the two Ti-related centers, resulting in a reduced capacitance of the space charge region of Ti^+-implanted samples (see curves 2 and 4 in Fig. 2). As a consequence, Ti(h)and Ti(k) have to

TABLE II. Ionization energies $\Delta E(i)$, capture cross sections $\sigma(i)$ of electrons and trap concentrations N(i) as obtained from an Arrhenius plot evaluation of centers Ti(h) and Ti(k), and ID_1 to ID_4 in the 4H SiC epilayer after Ti^+ implantation No. 1 and anneal.

Center i	Ionization energy $\Delta E(i)$ (meV)		Capture cross section $\sigma(i)$ (cm^2)		Concentration N(i) (cm^{-3})
	$\sigma \sim T^0$	$\sigma \sim T^{-2}$	$\sigma \sim T^0$	$\sigma \sim T^{-2}$	
Ti(h)	110	125	2×10^{-15}	1×10^{-14}	9×10^{14}
Ti(k)	150	170	3×10^{-15}	2×10^{-14}	2×10^{15}
ID_1	180	205	4×10^{-15}	3×10^{-14}	2×10^{14}
ID_2	185	210	1×10^{-17}	1×10^{-16}	6×10^{13}
ID_3	255	285	1×10^{-16}	1×10^{-15}	1×10^{14}
ID_4	370	405	1×10^{-14}	1×10^{-13}	2×10^{14}

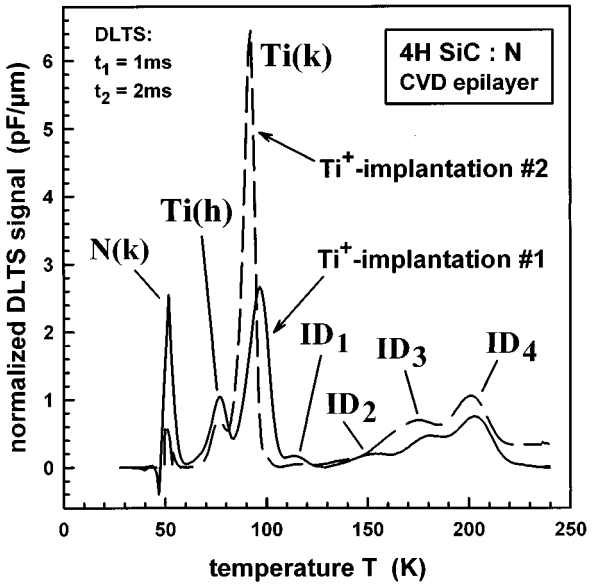

FIG. 3. Normalized DLTS spectra (time window $t_1=1$ ms/$t_2=2$ ms) taken on $4H$ SiC epilayers subsequent to Ti^+ implantation No. 1 (solid curve) and Ti^+ implantation No. 2 (dashed curve), respectively. The implanted epilayers were annealed at 1700 °C for 30 min.

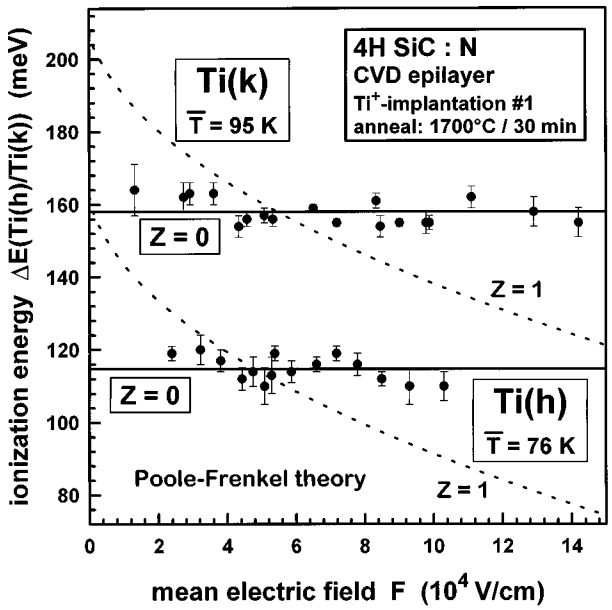

FIG. 4. Ionization energies $\Delta E[\mathrm{Ti}(h)]$ (lower part of the figure) and $\Delta E[\mathrm{Ti}(k)]$ (upper part of the figure) vs applied mean electric field F as obtained from double-correlated DLTS investigations. The solid/dotted lines are calculated with the Poole-Frenkel theory for a defect center with charge state $Z=0$ $(A^-\rightarrow A^0+e^-)/Z=1$ $(D^0\rightarrow D^++e^-)$ after emission of an electron and for a mean peak temperature of $T=76$ and 95 K, respectively (Ref. 17). The experimental data (full circles) are represented by the solid straight lines, meaning that centers Ti(h) and Ti(k) are acceptorlike.

act as acceptorlike centers, compensating partially the nitrogen donors in the temperature range from 50 to 140 K. This leads to a shift of the DLTS active zone to the trailing edge of the implanted Ti profile, resulting in reduced peak heights of Ti(h) and Ti(k) centers.

In order to prove that the Ti(h) and Ti(k) centers act as acceptors, we conducted double-correlated DLTS (DDLTS) investigations. The ionization energies $\Delta E[\mathrm{Ti}(h)]$ and $\Delta E[\mathrm{Ti}(k)]$ of these centers versus the mean electric field F as evaluated from the DDLTS measurements are shown in Fig. 4. It turns out that $\Delta E[\mathrm{Ti}(h)]$ and $\Delta E[\mathrm{Ti}(k)]$ are independent of the applied mean electric field (full circles). The solid horizontal straight lines and the dashed curves are calculated according to the Poole-Frenkel theory for centers, which are neutral ($Z=0$) and singly ionized ($Z=1$), respectively, in the final state.[17] The experimental data (full circles) fit well to the case $Z=0$. The considered defect centers are, therefore, uncharged after the emission of an electron, meaning that these centers are acceptorlike according to $A^-\rightarrow A^0+e^-$.

Opposite to the results obtained for the $4H$ polytype, we were not able to observe any corresponding Ti-related levels by DLTS in the $6H$ polytype. Figure 5 displays normalized DLTS spectra (time window $t_1=1$ ms/$t_2=2$ ms) of the as-grown (dot-dashed spectrum), the Ti^+-implanted (implantation No. 1, solid spectrum), and the V^+-implanted (dashed spectrum) $6H$ SiC epilayer. The three pronounced peaks ID_5–ID_7, which are observed in the spectrum of the Ti^+-implanted sample within the temperature range from 30 to 290 K, are also evident in the spectrum of the V^+-implanted sample. They are assigned to implantation-induced intrinsic defect centers comparable to those in $4H$ SiC (peaks ID_1–ID_4). The trap parameters of these peaks as obtained from an Arrhenius analysis are listed in Table III.

There is no feature detectable in the DLTS spectra of Fig. 5 that could be assigned to the nitrogen donor in $6H$, in contrast to the DLTS spectra taken on $4H$ SiC. This observation can be explained in terms of a differing freeze-out behavior of free electrons in $6H$. Curves 5 and 6 in Fig. 2 show that the strong freeze-out of electrons in $6H$ occurs already at $T=100$ K. This temperature position is slightly above the position where the nitrogen donor N(k_1,k_2) is detected by admittance spectroscopy in $6H$ SiC (see Ref. 18), and well above the temperature position where N(h) nitrogen donors are observed; as a consequence, nitrogen donors are not detectable in the DLTS spectra of $6H$ SiC. The concentration ratio of energetically deep N(k_1,k_2) nitrogen donors to the energetically shallower N(h) nitrogen donors of 2 to 1, as well as the slightly greater ionization energies of nitrogen donors [N(k_1,k_2), N(h)] in $6H$ SiC in comparison with the $4H$ polytype, are assumed to be responsible for the early freeze-out of free electrons in $6H$ SiC.

According to our DLTS results, we summarize that two Ti-related centers Ti(h) and Ti(k) are observable in $4H$ SiC, but no corresponding Ti-related centers can be detected in $6H$ SiC. The DDLTS investigations have revealed Ti(h) and Ti(k) to be acceptorlike defect centers.

The ionized Ti acceptor state $Ti^{3+}(3d^1)$ has previously been identified by ESR investigations of n-type $4H$ SiC bulk crystals.[8] Maier, Müller, and Schneider[8] pointed out that they could only detect an ESR spectrum of the $Ti^{3+}(3d^1)$ state in $4H$ SiC but not in $6H$ SiC. In order to explain this behavior, these authors suggested that the A^- ground state of the Ti

TABLE III. Ionization energies $\Delta E(i)$, capture cross sections $\sigma(i)$ of electrons and trap concentrations N(i) as obtained from an Arrhenius plot evaluation of centers ID_5 to ID_7 in the 6H SiC epilayer after Ti^+ implantation No. 1 and anneal.

Center i	Ionization energy $\Delta E(i)$ (meV)		Capture cross section $\sigma(i)$ (cm^2)		Concentration N(i) (cm^{-3})
	$\sigma \sim T^0$	$\sigma \sim T^{-2}$	$\sigma \sim T^0$	$\sigma \sim T^{-2}$	
ID_5	270	300	4×10^{-15}	3×10^{-14}	6×10^{14}
ID_6	395	430	2×10^{-14}	1×10^{-13}	1×10^{14}
ID_7	495	540	4×10^{-14}	3×10^{-13}	5×10^{14}

acceptor corresponds to a shallow level in the band gap of the 4H polytype close to the conduction-band edge, while its ground state in the 6H polytype is energetically already resonant in the conduction band. This suggestion is based on the empirical ''Langer-Heinrich-rule'' (Ref. 19) and the smaller band gap of the 6H polytype compared to the 4H polytype. Comparing our DLTS and DDLTS results with ESR findings, we propose that the two observed Ti-related centers Ti(h) and Ti(k) in 4H SiC are due to the ionized Ti acceptor state $Ti^{3+}(3d^1)$residing at hexagonal and cubic lattice sites, respectively. An assignment of the Ti(h) and Ti(k) acceptors to one of the two determined ionization energies cannot be met on the basis of our investigations; we also cannot decide whether Ti substitutes a Si or C site. Lee *et al.*[9] performed detailed ODMR studies on Ti acceptors in 4H SiC, and assigned the PL lines at 2.85 eV (B_0 line) and 2.79 eV (C_0 line) to Ti acceptors residing at hexagonal and cubic Si lattice site, respectively. Considering the Ti luminescence as a radiative recombination of an exciton bound to the Ti center proposed by Patrick and Choyke,[10] we conclude that the PL line located at higher energy corresponds to the Ti-related level which is energetically closer to the conduction band.

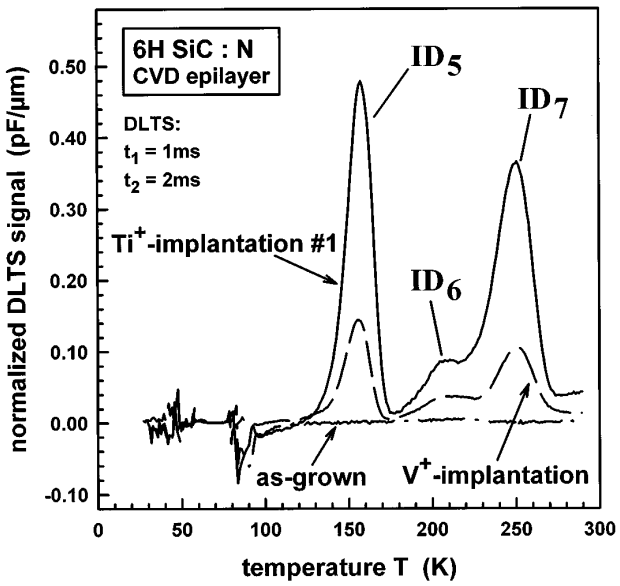

FIG. 5. Normalized DLTS spectrum (time window t_1=1 ms/ t_2=2 ms) of an as-grown (dot-dashed curve), of a Ti^+-implanted (implantation No. 1, solid curve), and of a V^+-implanted (dashed curve) 6H SiC epilayer. The implanted epilayers were annealed at 1700 °C for 30 min.

This means that the B_0 and C_0 lines correspond to the shallower $[E_C-(117\pm8)$ meV] and deeper $[E_C-(160\pm10)$ meV] Ti-related level, respectively. Taking into account the results of the ODMR investigations, the shallower and deeper Ti-related levels are due to Ti acceptors residing at hexagonal and cubic Si lattice sites.

The electrical activity of the implanted Ti acceptor achieved by an anneal at 1700 °C for 30 min is approximately 100%, as can be seen by comparing the concentration of Ti(k) centers which is not affected by the charge-carrier freeze-out (see Table II) with the implanted mean Ti concentration (see Table I). The experimental finding that the concentration of Ti(k) centers is equal to half of the implanted mean Ti concentration also supports our suggestion that the Ti(k) peak observed in the DLTS spectra corresponds to the substitutional Ti acceptor residing at cubic lattice sites.

In Fig. 6, the energy scheme for different SiC polytypes (4H, 6H, 15R, 21R, and 3C) and the ground-state energy of the ionized Ti acceptor $E[\mathrm{Ti}(k),(A^-/A^0)]$ in 4H SiC, as obtained from DLTS, are shown. The band-gap energy of the different polytypes listed in the figure is composed of the exciton band gap plus the binding energy of the free exciton of 27 meV,[20] which is assumed to be identical for all SiC polytypes considered. In order to make the figure transparent, we only depict the ground level of Ti acceptors residing at cubic lattice sites $[E(\mathrm{Ti}(k),(A^-/A^0)]$; however, identical conclusions are valid for the energetically shallower Ti acceptors residing at hexagonal lattice sites. This scheme is based on two essential assumptions: first, the empirical ''Langer-Heinrich rule''[19] is valid for the different SiC polytypes; and second, almost the complete band offset of the different SiC polytypes is connected with the conduction bands.

In III-V and II-VI compound semiconductors, Langer and Heinrich observed that levels of transition metals are aligned within a group of isovalent compound semiconductors with respect to a common bulk reference level.[19] As a consequence, the Ti acceptor level (A^-/A^0) determined in 4H SiC can be extended to further SiC polytypes at the same energy position as indicated in Fig. 6.

Regarding the band offsets between different SiC polytypes, internal photoemission investigations have been conducted on SiC/SiO_2 structures by Afanas'ev *et al.*[21] These authors stated that the upper valence-band edge of the investigated SiC polytypes (4H, 6H, 15R, and 3C) is energetically aligned within their measurement uncertainty of ±50 meV, which is indicated in Fig. 6 by the shadowed zone.

Evwaraye, Smith, and Mitchel[22] predicted a valence-band

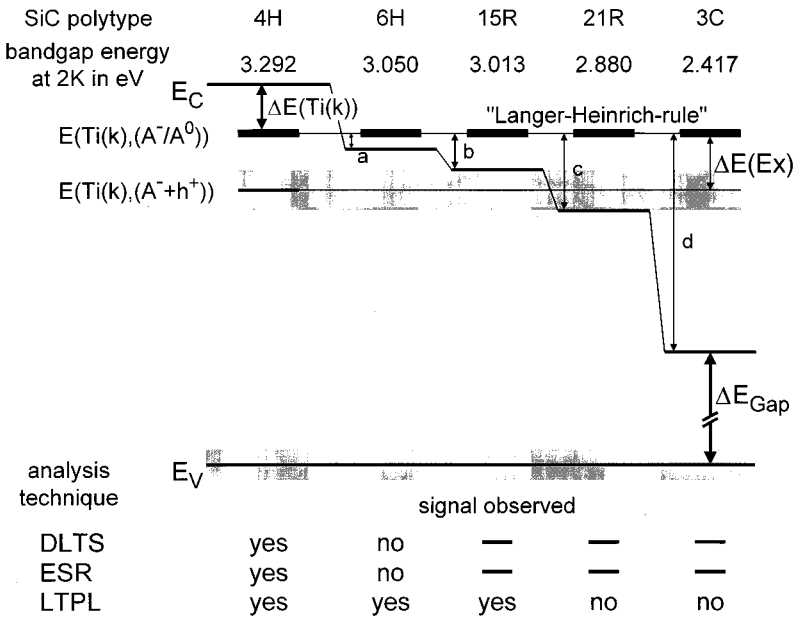

FIG. 6. Schematic energy diagram of five SiC polytypes ($4H$, $6H$, $15R$, $21R$, and $3C$) showing the ground-state level of the Ti(k) acceptor $E[\mathrm{Ti}(k),(A^-/A^0)]$ and the energy position of the Ti(k) acceptor after binding of an exciton $E[\mathrm{Ti}(k),(A^-+h^+)]$. It is assumed that the ''Langer-Heinrich rule'' is valid for the Ti acceptor level with respect to the different SiC polytypes. The table at the bottom of the figure summarizes whether a Ti-related signal can be obtained from the special analysis technique for the particular polytype (— means not yet checked, to our knowledge). Ionization energy of the Ti(k) acceptor in $4H$ SiC obtained from DLTS: $\Delta E[\mathrm{Ti}(k)]=(160\pm10)$ meV. Binding energy of the bound exciton $\Delta E(\mathrm{Ex})$ estimated from PL investigations on the $15R$ and $21R$ polytypes: 162 meV$\leqslant\Delta E(\mathrm{Ex})\leqslant$252 meV. (a) (82 $\pm$10) meV. (b) (119$\pm$10) meV. (c) (252$\pm$10) meV. (d) (715$\pm$10) meV.

offset between $4H$ and $6H$ SiC of about 170 meV from applying the ''Langer-Heinrich-rule'' to the vanadium donor level determined by optical admittance spectroscopy of $4H$ and $6H$ SiC. However, the measurement error of ±0.03 eV given in Ref. 22 for the determination of the band-gap energies of $4H$ and $6H$ SiC as well as for the vanadium donor level in $4H$ and $6H$ SiC leads to an overall error for the valence-band offset of ±120 meV; hence the results of Ref. 22 are no longer in contrast to the findings of Afanas'ev *et al.*

In addition, the theoretical work of Käckell, Wenzien, and Bechstedt[23] confirms the experimental results. From *ab initio* calculations, these authors obtained a valence-band offset of 0.03 eV and a conduction-band offset of 0.25 eV between $4H$ and $6H$ SiC, indicating that the predominant part of the band offset is connected with the conduction band. Based on these experimental findings and theoretical results, it is evident that the ground level of the ionized Ti acceptor $\mathrm{Ti}^{3+}(3d^1)$ among the considered polytypes ($4H$, $6H$, $15R$, $21R$, and $3C$) can only be observed in the $4H$ polytype.

According to Patrick and Choyke,[10] the Ti acceptor can bind an exciton leading to the $E[\mathrm{Ti}(k),(A^-+h^+)]$ level, which is lowered in energy by the binding energy $\Delta E(\mathrm{Ex})$ of the bound exciton with respect to the $E[\mathrm{Ti}(k),(A^-/A^0)]$ ground level (see Fig. 6). These authors reported PL lines due to the recombination of this bound exciton for the $4H$, $6H$, and $15R$ SiC polytypes; however, no radiative bound exciton recombination could be observed for the $21R$ and $3C$ SiC polytype. The energy position of the detected PL lines is largely independent of the SiC polytype, the number of observed no-phonon PL lines (A_0, B_0, C_0, etc.) depends on the particular polytype, and is correlated with the differing number of inequivalent lattice sites. Especially the fact that Ti-related PL lines are observed in the $15R$ polytype means that the $E[\mathrm{Ti}(h),(A^-+h^+)]$ and $E[\mathrm{Ti}(k),(A^-+h^+)]$ levels have to be located in the band gap of this polytype, while the corresponding levels of the $21R$ polytype are already resonant in the conduction band (see Fig. 6). Combining this observation with our DLTS results, we can estimate an energy range for the binding energy of the bound exciton $\Delta E(\mathrm{Ex})$, which is assumed to be independent of the SiC polytype and identical for Ti acceptors residing at hexagonal or cubic lattice sites:

$$162\ \mathrm{meV}\leqslant\Delta E(\mathrm{Ex})\leqslant252\ \mathrm{meV}.$$

Our discussion reveals that the available and independently obtained experimental results [DLTS (this work), ESR,[8] ODMR,[9] and PL (Ref. 10)] on the Ti acceptor in a series of SiC polytypes can be summarized in a model (see Fig. 6) which is able to explain all the experimental details. In contrast to Ti centers in Si, where Ti causes a strong recombination of free charge carriers by forming three deep levels with large capture cross sections[24] located in the forbidden band gap, it seems that Ti incorporated into SiC does not lead to such a strong degradation of the electrical properties. It turns out that Ti generates electrically active centers only in the $4H$ SiC polytype. There it is already observed in the as-grown CVD epilayers, and forms deep acceptors with moderate capture cross sections for electrons, which are of the order of 10^{-15} cm^2 (see Table II).

IV. SUMMARY

Based on our DLTS and DDLTS investigations and on ESR and PL results reported in the literature, we determined the ground-state levels of the ionized Ti acceptor $\mathrm{Ti}^{3+}(3d^1)/\mathrm{Ti}^{4+}(3d^0)\equiv A^-/A^0$ in $4H$ SiC to be equal to

$$E[\mathrm{Ti}(h)]=E_C-(117\pm8)\ \mathrm{meV},$$

$$E[\mathrm{Ti}(k)]=E_C-(160\pm10)\ \mathrm{meV};$$

the two differing levels are due to Ti atoms substituting for Si at hexagonal and cubic lattice sites, respectively. The assignment of the energy levels to hexagonal and cubic lattice sites is based on detailed ODMR investigations performed by Lee *et al.*[9] The ''Langer-Heinrich rule'' leads to the

suggestion that the corresponding Ti acceptor levels are resonant in the conduction band of the 6*H* SiC polytype and of all the other SiC polytypes with a band-gap energy $\Delta E_{\mathrm{Gap}} \leqslant \Delta E_{\mathrm{Gap}}(6H)$. Comparing Ti-related photoluminescence data of the 15*R* and 21*R* SiC polytype published by Patrick and Choyke,[10] and taking into account our DLTS results on Ti acceptors in 4*H* SiC, we can estimate a binding energy $\Delta E(\mathrm{Ex})$ of an exciton bound to the Ti acceptor: 162 meV $\leqslant \Delta E(\mathrm{Ex}) \leqslant$ 252 meV; it is assumed to be independent of the lattice site and the SiC polytype.

ACKNOWLEDGMENTS

The authors are indebted to Professor W. J. Choyke for many helpful and stimulating discussions on the Ti photoluminescence in SiC. The support of this work by the German Science Foundation (Sonderforschungsbereich 292), by the German Bundesministerium für Bildung, Wissenschaft, Forschung und Technologie (BMBF), and by the Swedish National Board for Industrial and Technical Development (NUTEK), is gratefully acknowledged.

[1] E. O. Johnson, RCA Rev. **26**, 163 (1965).
[2] R. W. Keyes, Proc. IEEE **60**, 225 (1972).
[3] K. Shenai, R. S. Scott, and B. J. Baliga, IEEE Trans. Electron Devices **ED-36**, 1811 (1989).
[4] B. J. Baliga, IEEE Electron Device Lett. **10**, 455 (1989).
[5] N. Nordell, S. G. Andersson, and A. Schöner, Inst. Phys. Conf. Ser. **142**, 81 (1996); N. Nordell, A. Schöner, and S. G. Andersson, J. Electrochem. Soc. **143**, 2910 (1996).
[6] H. Matsunami, Physica B **185**, 65 (1993); T. Kimoto, H. Nishino, W. S. Yoo, and H. Matsunami, J. Appl. Phys. **73**, 726 (1993).
[7] V. S. Vanier, V. A. Il'in, V. A. Karachinov, and Yu. M. Tairov, Fiz. Tverd. Tela (Leningrad) **28**, 363 (1986) [Sov. Phys. Solid State **28**, 201 (1986)].
[8] K. Maier, H. D. Müller, and J. Schneider, Mater. Sci. Forum **83-87**, 1183 (1992); K. Maier, Ph.D. thesis, Universität Freiburg, 1994.
[9] K. M. Lee, Le Si Dang, G. D. Watkins, and W. J. Choyke, Phys. Rev. B **32**, 2273 (1985).
[10] L. Patrick and W. J. Choyke, Phys. Rev. B **10**, 5091 (1974).
[11] K. Hölzlein, G. Pensl, M. Schulz, and P. Stolz, Rev. Sci. Instrum. **57**, 1373 (1986).
[12] J. R. Jenny, J. Skowronski, W. C. Mitchel, H. M. Hobgood, R. C. Glass, G. Augustine, and R. H. Hopkins, Appl. Phys. Lett. **68**, 1963 (1996).
[13] T. Kimoto, A. Itoh, H. Matsunami, S. Sridhara, L. L. Clemen, R. P. Devaty, W. J. Choyke, T. Dalibor, C. Peppermüller, and G. Pensl, Appl. Phys. Lett. **67**, 2833 (1995).
[14] W. Götz, A. Schöner, G. Pensl, W. Suttrop, W. J. Choyke, R. Stein, and S. Leibenzeder, J. Appl. Phys. **73**, 3332 (1993).
[15] *Semiconductors. Impurities and Defects in Group IV Elements and III-V Compounds*, edited by O. Madelung and M. Schulz, Landolt-Börnstein, New Series, Group III, Vol. 22, Pt. b, (Springer-Verlag, Berlin, 1989), p. 70.
[16] D. V. Lang, J. Appl. Phys. **45**, 3014 (1974).
[17] J. L. Hartke, J. Appl. Phys. **39**, 4871 (1968).
[18] S. E. Saddow, M. Lang, T. Dalibor, G. Pensl, and P. G. Neudeck, Appl. Phys. Lett. **66**, 3612 (1995).
[19] J. M. Langer and H. Heinrich, Phys. Rev. Lett. **55**, 1414 (1985).
[20] W. J. Choyke, in *The Physics and Chemistry of Carbides, Nitrides and Borides*, Vol. 185 of *NATO Advanced Study Institute Series*, edited by R. Freer (Kluwer, Dordrecht, 1990), p. 563.
[21] V. V. Afanas'ev, M. Bassler, G. Pensl, M. J. Schulz, and E. Stein von Kamienski, J. Appl. Phys. **79**, 3108 (1996).
[22] A. O. Evwaraye, S. R. Smith, and W. C. Mitchel, Appl. Phys. Lett. **67**, 3319 (1995).
[23] P. Käckell, B. Wenzien, and F. Bechstedt, Phys. Rev. B **50**, 10 761 (1994).
[24] K. Graff and H. Pieper, in *Semiconductor Silicon 1981*, edited by H. R. Huff, R. J. Kriegler, and Y. Takeishi (Electrochemical Society, Pennington, NJ, 1981), p. 331.